

See discussions, stats, and author profiles for this publication at: <https://www.researchgate.net/publication/334207653>

PALEOSOLS AND RELATED SOIL-BIOTA OF THE EARLY MIOCENE SANTA CRUZ FORMATION (AUSTRAL-MAGALLANES BASIN, ARGENTINA): A MULTIDISCIPLINARY APPROACH TO RECONSTRUCTING ANCIENT

Article in Latin American Journal of Sedimentology and Basin Analysis · July 2019

CITATIONS

13

12 authors, including:



María Sol Raigemborn

National Scientific and Technical Research Council

51 PUBLICATIONS 700 CITATIONS

[SEE PROFILE](#)

READS

380



Verónica Krapovickas

National Scientific and Technical Research Council

48 PUBLICATIONS 412 CITATIONS

[SEE PROFILE](#)



Alejandro Zucol

National Scientific and Technical Research Council

139 PUBLICATIONS 1,865 CITATIONS

[SEE PROFILE](#)



Luciano Zapata

Universidad Nacional de La Plata

7 PUBLICATIONS 76 CITATIONS

[SEE PROFILE](#)

Some of the authors of this publication are also working on these related projects:



Ichnology of desert systems [View project](#)



“Arqueología de ambientes acuáticos del Centro-este argentino” (UNLP-Código 11/N770) [View project](#)

PALEOSOLS AND RELATED SOIL-BIOTA OF THE EARLY MIocene SANTA CRUZ FORMATION (AUSTRAL-MAGALLANES BASIN, ARGENTINA): A MULTIDISCIPLINARY APPROACH TO RECONSTRUCTING ANCIENT TERRESTRIAL LANDSCAPES

M. Sol Raigemborn^{1,2,*}, *Verónica Krapovickas*³, *Alejandro F. Zucol*⁴, *Luciano Zapata*⁵, *Elisa Beilinson*^{1,6}, *Nestor Toledo*⁷, *Jonathan Perry*⁸, *Sabrina Lizzoli*¹, *Lucía Martegani*⁹, *David E. Tineo*^{1,10}, *Esteban Passeggi*⁴

¹ CONICET - UNLP. Centro de Investigaciones Geológicas, Diagonal 113 Nº 275 (1900) La Plata, Argentina.

² Cátedra de Micromorfología de Suelos, Facultad de Ciencias Naturales y Museo, UNLP, Calle 122 y 60 s/n, (1900) La Plata, Argentina.

³ IDEAN - CONICET, Departamento de Ciencias Geológicas, FCEyN, UBA, Ciudad Universitaria, Pab. 2, (C1428EHA) Buenos Aires, Argentina.

⁴ Laboratorio de Paleobotánica, Centro de Investigaciones Científicas y Transferencia de Tecnología a la Producción (CICYTTP-UADER Provincia de Entre Ríos - CONICET), Dr. Materi y España SN, E3105BWA, Diamante, Argentina.

⁵ Cátedra de Fundamentos de Geología, Facultad de Ciencias Naturales y Museo, UNLP, Calle 122 y 60 s/n (1900) La Plata, Argentina.

⁶ Cátedra de Sedimentología Especial, Facultad de Ciencias Naturales y Museo, UNLP, Calle 122 y 60 s/n (1900) La Plata, Argentina.

⁷ División Paleontología Vertebrados, Unidades de Investigación, Anexo Museo, Facultad de Ciencias Naturales y Museo, Avenida 60 y 122, 1900, La Plata, Argentina. CONICET.

⁸ Center for Functional Anatomy and Evolution, The Johns Hopkins University School of Medicine, Baltimore, USA.

⁹ Cátedra de Mineralogía, Facultad de Ciencias Naturales y Museo, UNLP, Calle 122 y 60 s/n (1900) La Plata, Argentina.

¹⁰ Cátedra de Geología de Combustibles, Facultad de Ciencias Naturales y Museo, UNLP, Calle 122 y 60 s/n (1900) La Plata, Argentina.

* msol@cig.museo.unlp.edu.ar

ARTICLE INFO

Article history

Received December 10, 2018

Accepted June 8, 2019

Available online June 10, 2019

Invited Editor

José I. Cuitiño

Handling Editor

Sebastian Richiano

Keywords

Pedotypes

Ichnofossils

Phytoliths

Vertebrates

Santa Cruz Province

ABSTRACT

The middle and upper parts of the lower Miocene Santa Cruz Formation (~17–15.9 Ma) in the southeastern Austral-Magallanes Basin (southern Patagonia, Argentina) crop out as a fluvial succession that in parts is pedogenically modified. The study of the paleosols of this unit combined with the study of ichnofossils, microremains, and fossil vertebrates present in these allows us to reconstruct past environmental, ecological, and climatic conditions, as well as paleolandscape evolution of the Santa Cruz Formation during ~1 my. These reconstructions demonstrate three different stages during which very weak to moderate pedogenesis took place. The first one (middle part of the unit) is an epiclastic distal floodplain bearing Calcisols or paleo-calcic Inceptisols, which record a relatively dense vegetation integrating trees, shrubs, palms, and short grasses. Soil fauna is scarce and it is in association with a vertebrate fauna typical of coastal “Santacrucian assemblages”. The second landscape stage (the bottom of the lowermost upper part of the unit) is composed of epiclastic distal floodplain areas and minor pyroclastic proximal floodplain settings that contain mainly Vertisols. Vertisols record an ecosystem dominated by grasses and palms adapted to variable conditions in hydric availability (C_4 plants) and by solitary bee larvae, and adult and nymph soil beetles. Finally, up-section, the third stage attests to the existence of an epiclastic and pyroclastic distal and proximal floodplain over which Protosols developed. Past ecosystems supported grass vegetation (C_3 plants), oligochaete annelids and a moderately diverse insect soil fauna (interpreted by their trace fossils) composed of solitary bee larvae, soil beetles and their pupae, cicada nymphs, and myriapods. This combined abiotic (paleosols) and biotic (ichnofossils, microremains, and vertebrates) study indicates

that several factors controlled the landscape evolution during the early Miocene of southeastern Patagonia. Highly aggrading fluvial conditions, variations in the position in the floodplain and in sedimentation/pedogenesis ratio, the input of pyroclastic materials, the length of landscape stability, changing hydrologic conditions, and fluctuations of wetter and drier phases in a context of relatively warm and humid climate, seem to be the main factors controlling the landscape.

INTRODUCTION

Paleosols and their constituents, including ichnofossils and microremains such as phytoliths, together with the fossil fauna preserved in these soils, can be helpful tools to interpret paleoenvironmental, paleoecological, and paleoclimatic conditions in continental settings (e.g., Kraus and Hasiotis, 2006; Sheldon and Tabor, 2009; Hembree and Bowen, 2017). This is because the soil development is influenced, among other things, by environmental factors such as climate and organisms (e.g., Retallack, 2001; Buol *et al.*, 2011). At the same time, as ichnofossils (structures biologically produced *in situ* that result from the movement of organisms through or on a medium) respond directly to the environment in which they formed, they can be thought of as representatives of the environments in which they are preserved (Bromley, 1996). Similarly, phytoliths (microscopic silica particles formed inside living plants) preserved within paleosols provide the record of vegetation composition and allow ecosystem reconstructions (e.g., Zucol *et al.*, 2018). In addition, the analysis of vertebrate fauna from paleosols leads to the understanding of paleoecological conditions (e.g., presence of taxa adapted to open and arid environments or adapted to vegetated and humid ones). Thus, the association of paleosols, ichnofossils, and phytoliths—together with fossil mammals—provide direct and complementary evidence of ancient terrestrial landscapes from both biotic and abiotic perspectives (e.g., Retallack, 2001; Kraus and Hasiotis, 2006; Hasiotis and Platt, 2012; Kohn *et al.*, 2015; Catena *et al.*, 2016, 2017; Hembree and Bowen, 2017; Badawy, 2017).

The Santa Cruz Formation (SCF) is an upper lower Miocene unit of estuarine to fluvial origin that crops out widely in the Austral-Magallanes Basin (southern Patagonia, Argentina) (e.g., Raigemborn *et al.*, 2015; Cuitiño *et al.*, 2016a). The SCF has been widely studied since the 19th Century due to the richness

in fossil mammals (Santacrucian South American Land Mammal Age) (see Vizcaíno *et al.*, 2012 for a review). These paleontological (faunal and vegetational) studies and their paleoenvironmental reconstructions were mainly constrained to the lower part of the unit, which crops out along the Atlantic coastal cliffs in southern Santa Cruz Province (Fig. 1A) (e.g., Tauber, 1994, 1997a, 1997b; Kay *et al.*, 2008, 2012; Brea *et al.*, 2012, 2017; Zucol *et al.*, 2015; Crifò *et al.*, 2016, 2017, 2018). In the last few years, environmental reconstructions based on sedimentological and ichnological analysis of the entire unit have been published (Krapovickas, 2012; Matheos and Raigemborn, 2012; Raigemborn *et al.*, 2015; Cuitiño *et al.*, 2016b; Zapata *et al.*, 2016; Zapata, 2018). These studies have highlighted the occurrence of subtropical environments with a vegetation mosaic of open and closed habitats that occupied fluvial environments. Meanwhile, the middle and upper parts of the unit seem to record the existence of environments adapted to more arid and seasonal conditions than those prevailing during the deposition of the lower part of the SCF. However, pedological, ichnological, and phytolithic analyses of the SCF in the southernmost part of Santa Cruz Province, and past environmental reconstructions based on these studies are still very scarce (Krapovickas, 2012; Zapata *et al.*, 2016; Raigemborn *et al.*, 2018a). Similarly, with the exception of Tauber's work (see above), Santacrucian fossil faunas in this area of the basin have never been studied in detail. Therefore, a combined paleopedological, ichnological, and paleobotanical analysis of the SCF supported by paleontological studies, represents a potential archive of data to complement previous environmental interpretations and allows us to test changing terrestrial conditions. This contribution interprets the early Miocene environments in the south of the Santa Cruz Province (Austral-Magallanes Basin) and reconstructs terrestrial landscapes based on an integrated abiotic-biotic study of the middle and upper parts of the SCF.

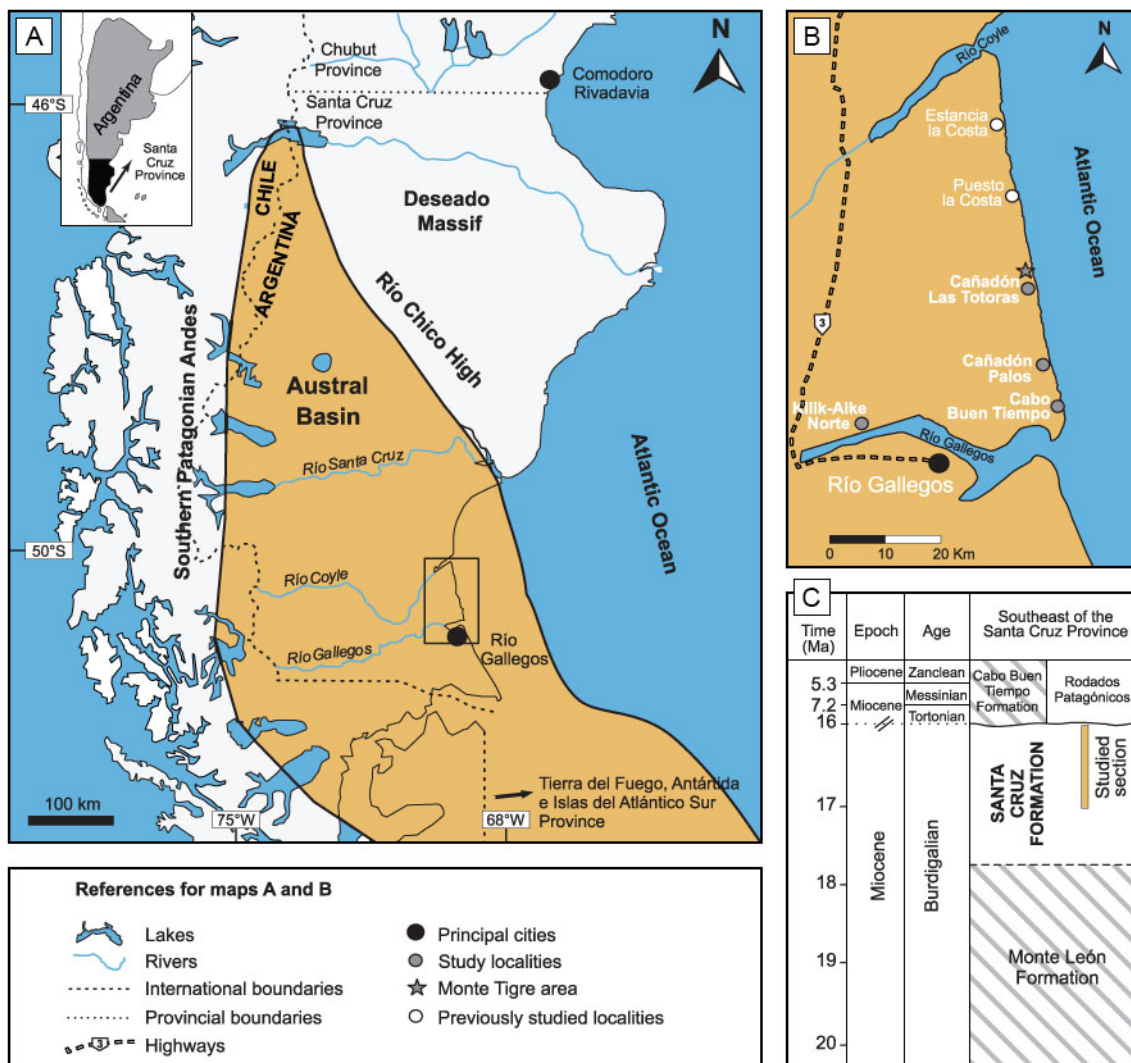


Figure 1. a) Map showing position and boundaries of the Austral-Magallanes Basin (after Biddle *et al.*, 1986), and position of the study localities (rectangle). b) Location of the analyzed sections of the Santa Cruz Formation and previously studied ones. c) Stratigraphic chart of the southeast Santa Cruz province with the position of the studied interval (modified from Raigemborn *et al.*, 2018a). It extends through continental (white) and marine (striped) units.

GEOLOGICAL AND SEDIMENTOLOGICAL BACKGROUND

The Austral-Magallanes Basin is located in southernmost South America (Fig. 1A–B). During its foreland stage (Cretaceous and Cenozoic), the basin was infilled with marine sediments deposited during several Atlantic transgressions that were intercalated with intervals of non-deposition, erosion, and continental deposition (Biddle *et al.*, 1986; Malumián, 1999). In particular, during the lower Miocene the basin was infilled with the marine deposits of the Monte Léon Formation (Bertels, 1970) and equivalent units, which were transitionally succeeded by the

early Miocene estuarine and fluvial deposits of the SCF (Matheos and Raigemborn, 2012; Raigemborn *et al.*, 2015). The upper Miocene–Pleistocene marine and glaciofluvial sediments of the Cabo Buen Tiempo Formation (Hatcher, 1897) and the “Rodados Patagónicos” (Fidalgo and Riggi, 1970) (Fig. 1C) disconformably overlie the SCF. The SCF in the Atlantic coastal cliffs of southern Santa Cruz Province (Fig. 1B) is a ~225 m-thick succession composed mainly of stacked fluvio/alluvial deposits intercalated with paleosols (Genise and Bown, 1994; Tauber, 1994; Matheos and Raigemborn, 2012; Raigemborn *et al.*, 2015; Zapata *et al.*, 2016; Zapata, 2018). In the lower part of the unit an estuarine environment was formed

(Raigemborn *et al.*, 2015; Cuitiño *et al.*, 2016a; Parras and Cuitiño, this volume). Tauber (1994, 1997a, 1997b) divided the SCF into two members based on lithological aspects, separated by a locally erosional discontinuity: the lower Estancia La Costa Member, dominated by pyroclastic and epiclastic mudrocks, and the upper Estancia La Angelina Member, dominated by epiclastic muddy and sandy deposits. Recently, sedimentological analysis of the Atlantic SCF south of Río Coyle, allowed Zapata (2018) to differentiated five sections: I, II, III, IV, and V (see below). Sections I–III correspond to the Estancia La Costa Member; meanwhile sections IV–V are equivalent to the Estancia La Angelina Member.

In the study area (Cañadón Las Totoras, Cañadón Palos, Cabo Buen Tiempo, and Killik-Aike Norte localities, Fig. 1B), the SCF outcrops are 15–90 m thick and are exposed mainly along the sea cliffs. The outcrops of the SCF studied in this contribution correspond to the middle part of the unit (*i.e.*, the upper part of the Estancia La Costa Member, or section III of Zapata, 2018), and to the upper part of the unit (*i.e.*, the Estancia La Angelina Member, or sections IV and V). Middle and upper parts of the SCF range in age from ~ 17.0 to 15.9 Ma (Perkins *et al.*, 2012; Fig. 1C). In these studied localities, the base of the SCF is not exposed and its top is truncated by the “Rodados Patagónicos” or by the Cabo Buen Tiempo Formation (Figs. 1C and 2).

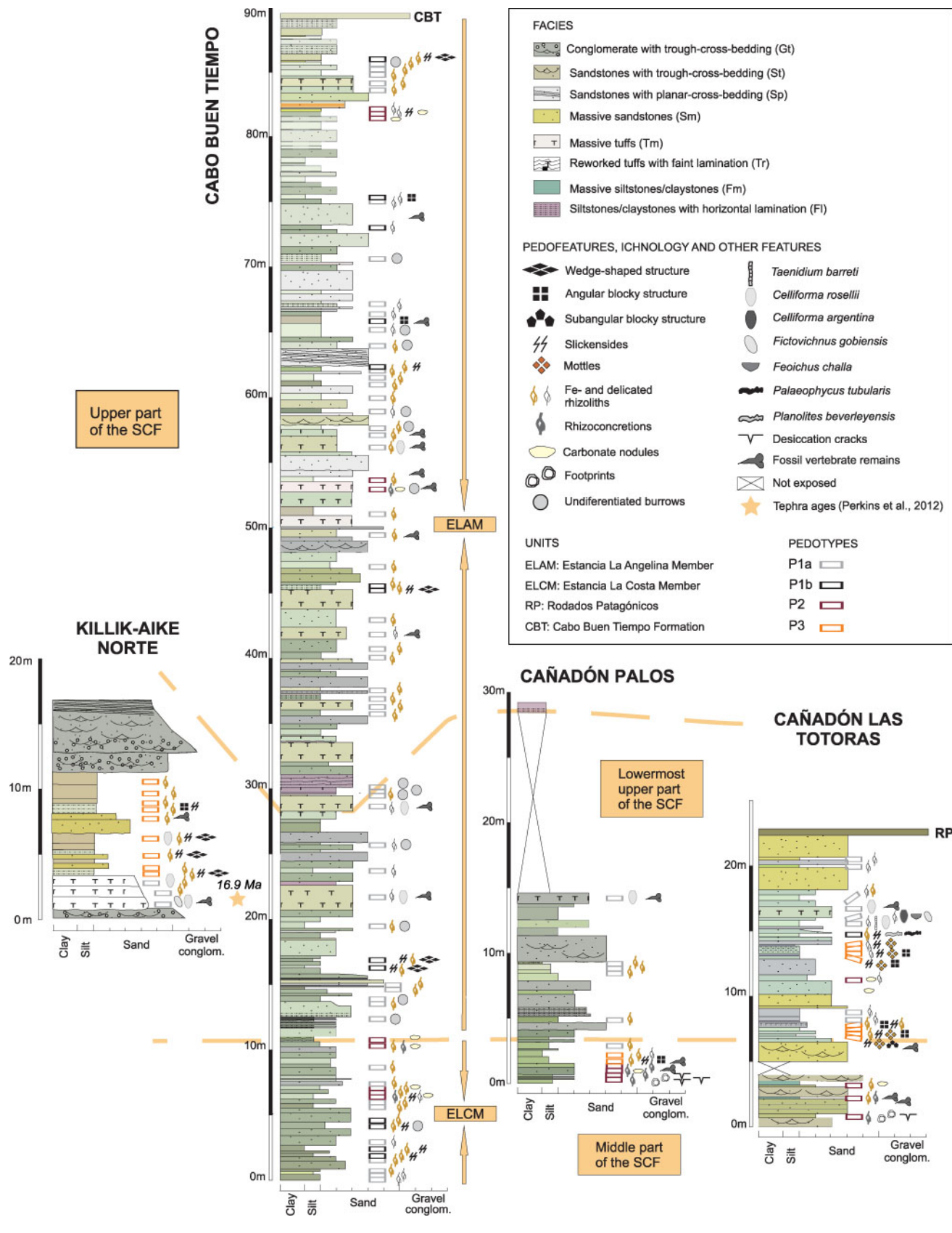
According to Zapata (2018), sections III, IV and V of the SCF are predominantly made up by floodplain deposits frequently affected by pedogenesis. These deposits show a distinct lithological change between section III and sections IV–V, from epiclastic (Sm, Fm and Fl facies) to pyroclastic with varying degrees of epiclastic participation (Tm, Tr, Sm, Fm and Fl facies; see Table 1 and Fig. 2). Zapata (2018) also characterized the fluvial channel styles that develop in each section, all of which are composed by coarse-grained beds (Gt, St and Sp facies; see Table 1 and Fig. 2) regardless of their stratigraphic location. Even though all the studied sections of the SCF correspond to moderate–high energy fluvial systems, important geometric and architectural differences can be distinguished between them. Section III channels show broad ribbon and narrow sheet-like morphologies, interpreted as confined and unconfined simple channels. Section IV channels can be described as narrow and broad ribbons, and narrow sheets interpreted mainly as confined simple channels, and in

less proportion as unconfined simples and confined complex channels. Section V channels show broad and narrow ribbon-like morphologies, and were interpreted as confined, laterally stable, simple channels by Zapata (2018).

METHODS AND SAMPLES

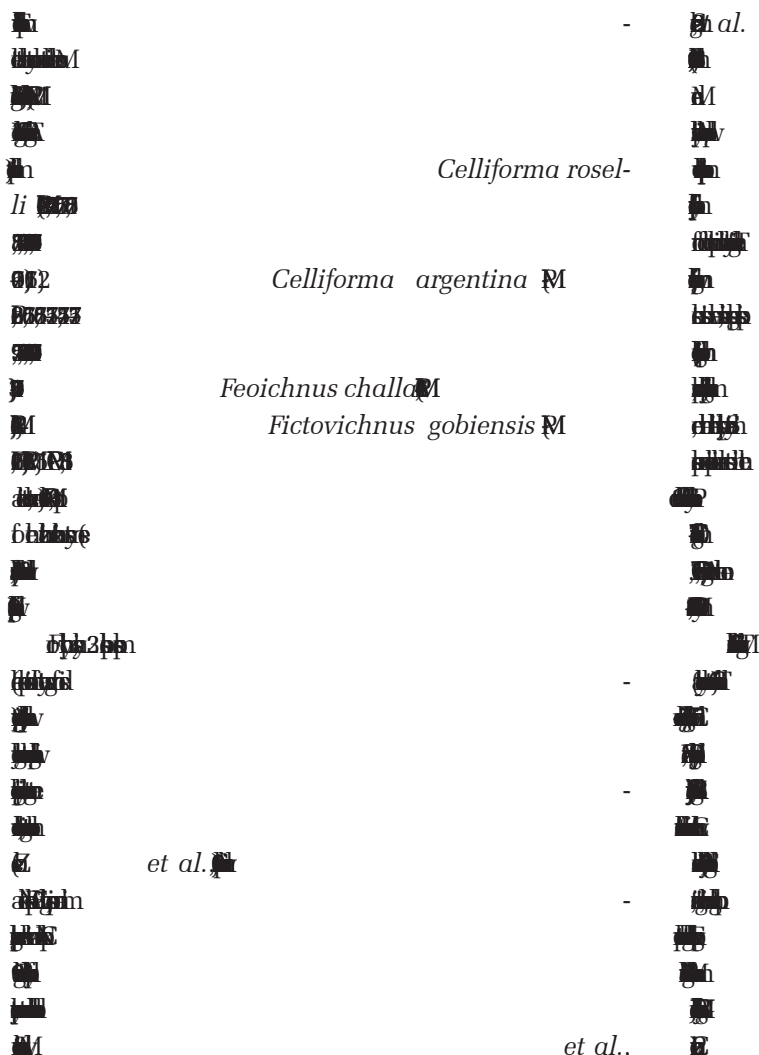
Ichnofossils and the paleosols that contain them were sampled in the study area at the four localities mentioned before. Paleosols were identified in outcrop based on macroscopic pedofeatures such as structure, mottles, nodules, color, slickensides, as well as rhizoliths and other trace fossils (*e.g.*, Retallack, 2001) (Fig. 2). For each paleosol horizon, thickness, contact types, mineral composition, mean grain size, ped structure, type of nodules, and evidence of bioturbation were described (*e.g.*, Retallack, 2001; Schoeneberger *et al.*, 2012). Colors were described according to the Munsell notation (Munsell Soil Color Book, 2013). Additionally, a micromorphological analysis was also undertaken. Thin sections of paleosol matrix were studied in order to establish mean grain size, mineralogical composition, porosity, microstructure, pedofeatures, fine material (groundmass), and microfabrics. Here we applied the criteria of Bullock *et al.* (1985), Stoops (2003), and Stoops *et al.* (2010). Selected paleosols were collected to determine clay composition. Clay mineralogy was determined from X-ray diffraction (XRD) pattern. The methodology used for sample preparation and semi-quantification of the minerals follows Raigemborn *et al.* (2014). Analyses were run on a PANalytical X'Pert PRO diffractometer (Centro de Investigaciones Geológicas, La Plata, Argentina), using Cu radiation ($K\alpha = 1.5 \text{ \AA}$) and a Ni filter, with generation settings of 40 kV and 40 mA. Routine air-dried mounts were run between 2 and 32 $^{\circ}\text{2}\theta$ at a scan speed of 2 $^{\circ}\text{2}\theta/\text{min}$. Samples were ethylene glycol-solvated without saturation pre-treatment and heated to 550 $^{\circ}\text{C}$. Then they were run from 2 to 27 $^{\circ}\text{2}\theta$ and 3 to 15 $^{\circ}\text{2}\theta$, respectively, at a scan speed of 2 $^{\circ}\text{2}\theta/\text{min}$. Paleosol classification was based on macro- and micromorphological features recognized in the constituent horizons, and on mineralogical analysis (XRD) through a comparison with the USDA (United State Department of Agriculture) soil taxonomy (Soil Survey Staff, 1999; Schoeneberger *et al.*, 2012) and with the paleosol classification of Mack *et al.* (1993).

The trace fossils studied are mostly preserved



Facies code	Features	Interpretation	Associated pedotypes
Gt, St, Sp	Fine-grained conglomerate to medium-grained sandstones with trough/planar cross-bedding.	Simple and complex (confined and unconfined) channels	-
Sm	Medium–very fine massive sandstones	Non-channelized sandy sheetfloods of the proximal–distal floodplain	P1a, P1b, P2, P3
Tr	Medium–fine reworked tuffs with faint lamination	Unconfined pyroclastic sheetfloods in the proximal floodplain	P1a, P1b
Tm	Massive very fine tuffs	Ash-fall deposits in distal floodplain settings	P1a, P1b, P2, P3
Fm	Massive siltstones–claystones	Suspension fallout in still-stand water in the distal floodplain	P1a, P1b, P2, P3
F1	Siltstones–claystones with horizontal lamination	Deposition from suspension and from traction currents in distal floodplain areas	P1a, P1b,

-



Celliforma roselli
et al. 2014

Celliforma argentina M

Feoichnus chalame

Fictovichnus gobiensis M

et al. 2014

et al., 2014

GENERAL FEATURES OF THE PALEOSOLS OF THE SANTA CRUZ FORMATION

Paleosols of the SCF crop out in the study area as continuous tabular beds, pale greenish yellow to grayish olive in color, and defined pedogenic horizons can be recognized in them (Fig. 2). Internally, these horizons are mainly massive or they show variations in the arrangement of soils aggregates ranging from incipient to well-defined wedge-shaped to angular-subangular blocky structure (Fig. 2). In a few cases, a relict primary lamination was recognized. The most conspicuous macropedofeatures are ferric and delicate rhizoliths, and slickensides (Fig. 2). Mottles, carbonate rhizoliths, and desiccation cracks are less frequent (Fig. 2). Abundant vertebrate fossil remains also occur, as well as invertebrate and vertebrate trace fossils (Figs. 2 and 3).

ICHNOFOSSILS OF THE SANTA CRUZ FORMATION

Celliforma rosellii Genise and Bown, 1994

This trace fossil mostly comprises indurated internal molds of isolated breeding or nidification chambers (Callichnia). Cells are oval shaped, with one rounded end and one flattened end. They have a smooth lining and lack discrete walls and antechambers (Fig. 3A). The dimensions of the internal mold cell are 1.3–2.3 cm long and 0.7–1.2 cm-wide, coincident with the type material described from the same unit. Some cells record a basal area of different coloration that represents the exceptionally preserved semiliquid food provision for the developing bee larva (Fig. 3A) (Zapata *et al.*, 2016).

Celliforma argentina Zapata *et al.*, 2016

As with *C. rosellii*, *Celliforma argentina* consists of single isolated chambers in a vertical orientation without antechambers and with discrete walls (Genise, 2000; Zapata *et al.*, 2016). In particular, the *C. argentina* comprise an internal mold of barrel shape; the inferior end of the chamber is rounded to flattened. By contrast, in *C. rosellii* the inferior end of the chamber is rounded to pointed, producing an oval shape for the whole cell. In addition, in *C. argentina* the dimension of the cells is markedly smaller than in *C. rosellii*: in complete specimens of *C. argentina*, the length seldom if ever exceeds 1.1 cm (Fig. 3B). Mean

length for SCF specimens of this ichnospecies is 0.9 cm and mean diameter is 0.5 cm. The difference in size between the two ichnospecies of *Celliforma* could indicate that these trace fossils were made by two different bee taxa. As the brood cells are produced by adults, it is clear that the material does not correspond to ontogenetic series. In addition, intraichnospecific size variation within *C. argentina* do not overlap with that expressed by *C. rosellii*.

Feoichnus challa Krause *et al.*, 2008

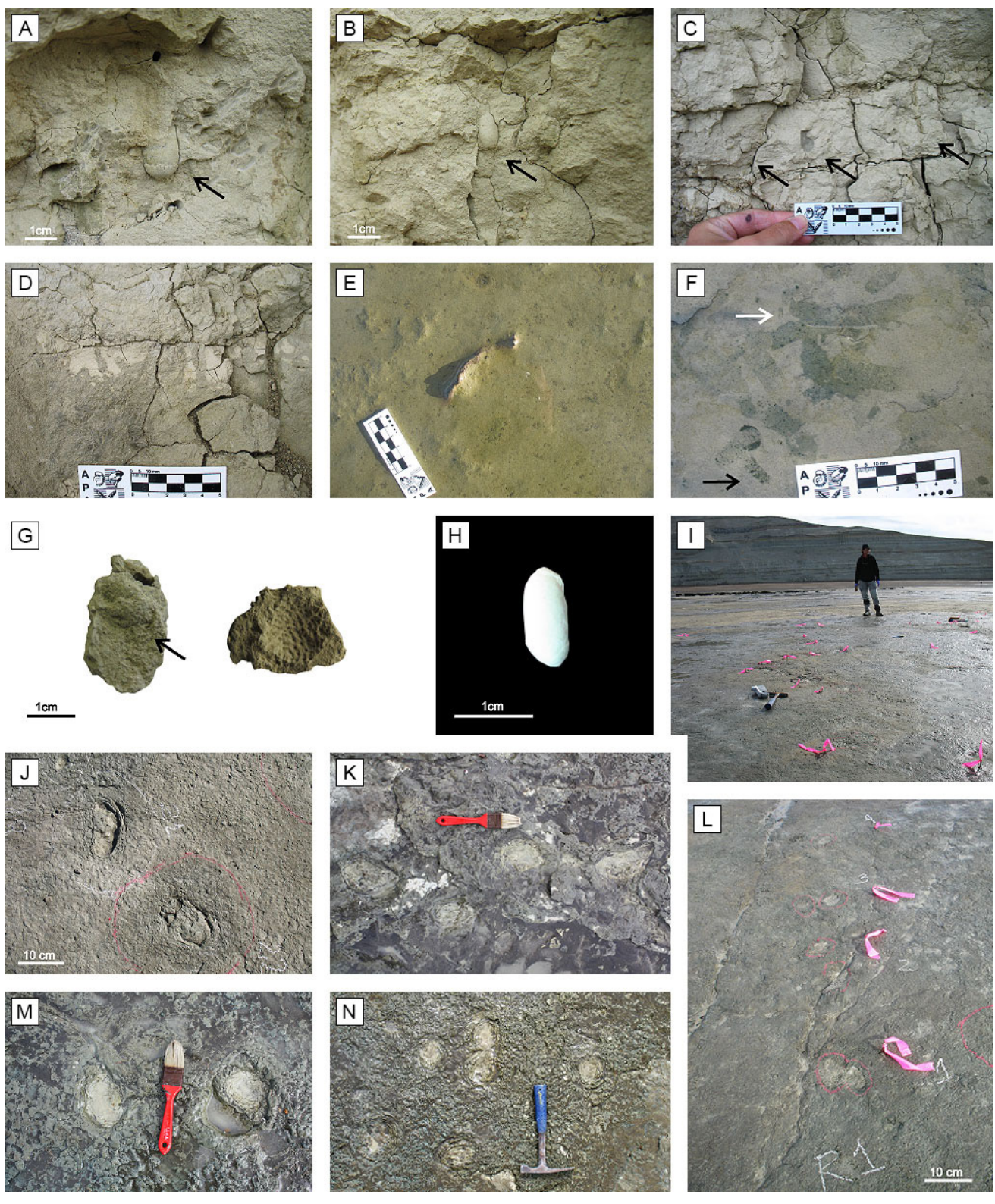
The trace fossil consists of an unfilled hemispherical, upwardly concave, dish-shaped structure attributed to a cicada nymph feeding chamber. The internal surface is smooth with irregularly distributed pits and scratches while the external surface is rough and irregular, without ornamentation (Fig. 3G). The preservation of only the base (dish-shaped structure) of the chamber results from the drainage of anal secretions held in the chamber and the impregnation of the surrounding soil particles, with pedogenic processes precluding the preservation of the rest of the chamber. Finally, the pits correspond to impression of the legs of the producer. In the best preserved specimen the external diameter is 1.4 cm, the height is 0.6 cm and the depth is 0.2 cm. The wall thickness varies at the base from 1 to 3 cm and the lateral wall is 0.3 cm thick.

Fictovichnus gobiensis Johnston *et al.*, 1996.

These trace fossils correspond to internal cast of chambers that are ellipsoid to ovoid in shape with a smooth internal surface and no wall. Both ends of the chambers are rounded and lack terminal, sub-terminal, or medial scars (Fig. 3H). They correspond to pupal chambers of beetles that pupate in the soil such as Scarabaeidae, Tenebrionidae, and Curculionidae (Johnston *et al.*, 1996). The chambers are 0.84–0.95 cm long and 0.42–0.45 cm wide. The SCF material would mainly correspond to failed cocoons as they are mostly preserved as complete chambers (Zapata *et al.*, 2016). Only two specimens were collected although many were recorded *in situ* at Killik-Aike Norte locality.

Palaeophycus tubularis Halls, 1847.

This trace fossil consists of simple dwelling bur-



argentina
Palaephycus tubularis
Taenidium barrettii **Palaephycus tubularis**
challae

C. argentina, C. rosellii
Planolites beverleyensis

Ictovichnus gobiensis

Celliforma rosellii
Celliforma
Feoichnus

with a tapered anterior margin, roughly 15 cm long and 10 cm wide; 4) medium circles approximately 8 cm in diameter; 5) small sub-oval footprints, 6 cm long and 5 cm wide; 6) small sub-circular footprints, 5 cm in diameter (Krapovickas *et al.*, 2013). These morphological characteristics, together with a very well-known mammalian fauna, permit reasonable inferences about the producers of the traces. In the case of 1 and 3, the producer could be assigned to terrestrial ground sloths such as Megatherioidea or Mylodontidae (Xenarthra, Folivora). This is mostly based on the presence of a (presumably medial) concave curvature associated with the lateral rotation of the foot (Krapovickas *et al.*, 2009). Large sub-circular footprints (2) have a size range and outline that could correspond to macrauchenids, toxodontids, and gliptodonts. The medium circular footprints (4) were assigned to medium sized toxodontids (Krapovickas *et al.*, 2013). Small sub-oval footprints (5) are comparable with those produced by protherotherids (Krapovickas *et al.*, 2009). Finally, small sub-circular footprints (6) have a size range comparable with those of typhotherid notoungulates.

Root traces

A variety of root traces (rhizoliths *sensu* Klappa, 1980) is preserved in the analyzed SCF. They include, following Krapovickas (2012), mainly (1) delicate root traces, (2) ferric root traces, (3) haloed root traces, and (4) calcareous rhizoconcretions.

Delicate or filamentous root traces are 0.05–0.3 cm in diameter. They taper downwards and lack infill, probably owing to selective erosion of the infilling material. Ferric root traces have a red to yellow-brown color within the root infill and on its margins (Fig. 3C). The red and yellow-brown colors result from a mixture of iron oxides (hematite and goethite). A redder color indicates more hematite (e.g., Schwertmann and Taylor, 1977; Kraus and Hasiotis, 2006). Ferric root traces vary from delicate or filamentous to those with greater size and diverse branching pattern. Some consist of vertical primary roots that taper downwards (0.5–0.2 cm wide) and have secondary roots (0.1–0.2 cm wide) that branch downwards with an inclination of 45 degrees. Others, have an almost constant diameter subtly tapering downwards from 0.7 to 0.4 cm with horizontally inclined secondary root traces. Haloed root traces represent delicate rhizoliths with drab

haloes extending out into the paleosol matrix (Fig. 3C). Carbonatic rhizoconcretions are mainly vertically disposed tubular structures that comprise concentric layers of carbonate deposited on the ancient root margins (rhizosphere), with a central hole filled by the host sediment, where the ancient root was located (Raigemborn *et al.*, 2018a).

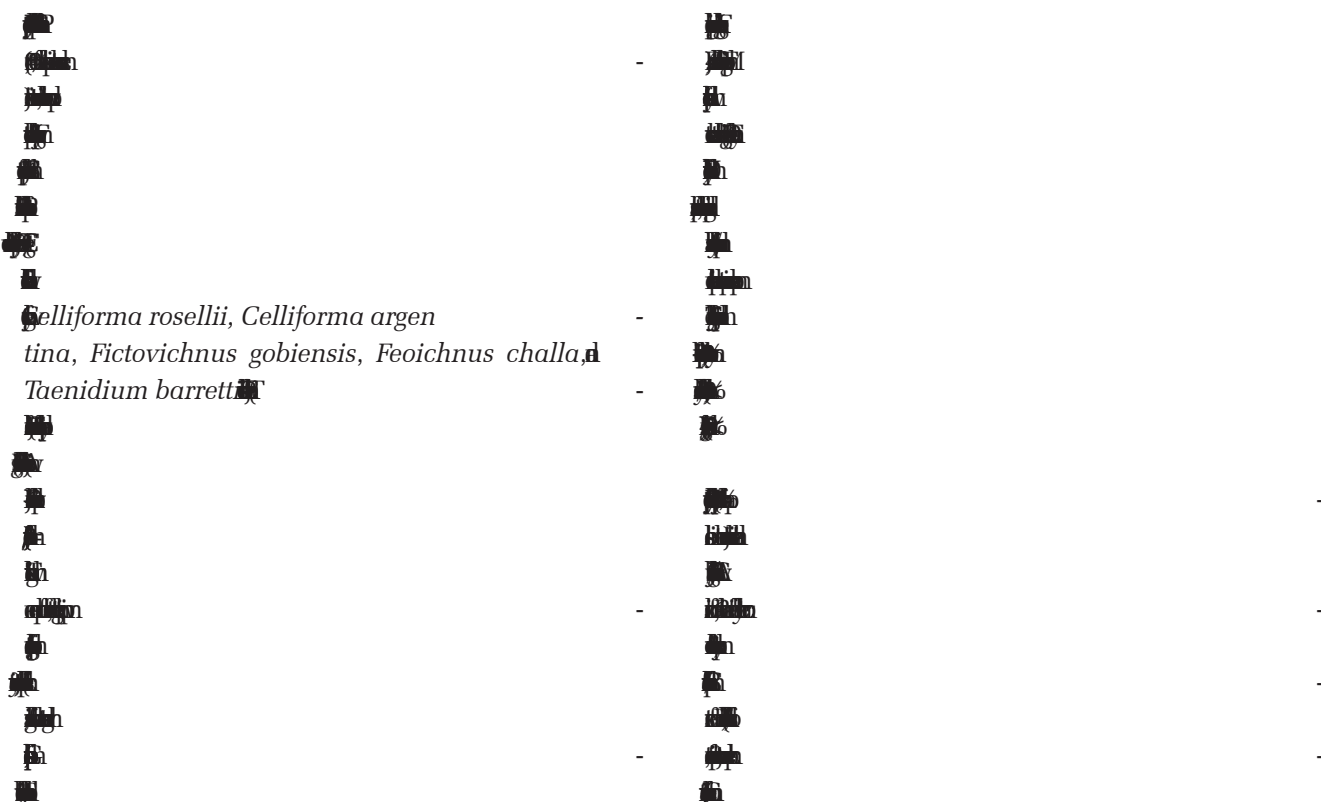
PALEOSOL TYPES OF THE SANTA CRUZ FORMATION

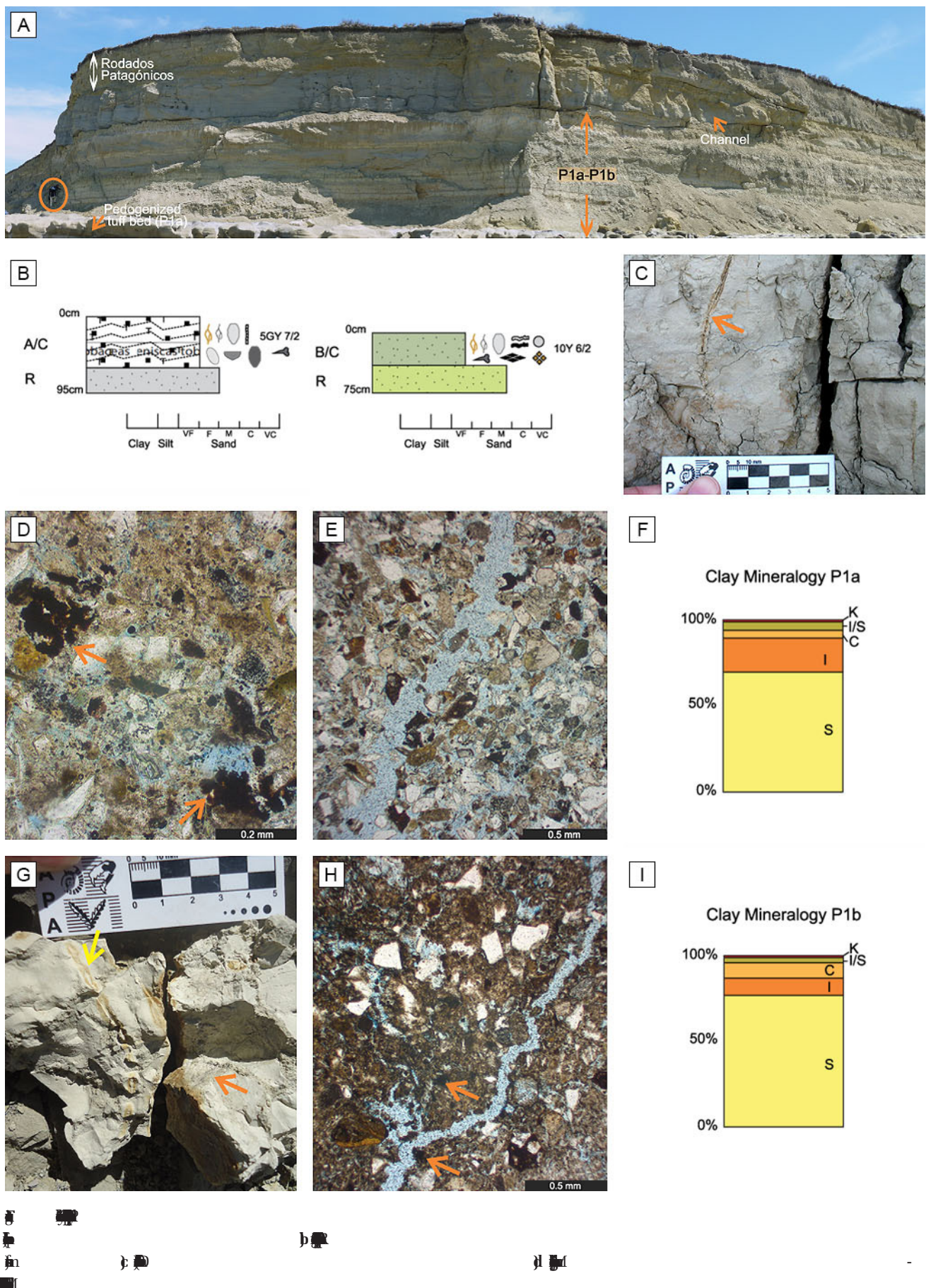
From a total of 116 pedogenically modified beds recognized through the analyzed profiles of the SCF in the study area, three paleosol types (pedotypes) were defined (Figs. 2, 4, 5 and 6; and Table 2). Surface A horizons, where paleosols were not removed by erosion, are recognized in bioturbated beds. The sub-surface Bk horizons are defined by how they reflect the concentration of pedogenic carbonate (rhizoconcretions and/or nodules). The Bss designation represents a horizon that has abundant slickensides. Basal C or R horizons are assigned based on having little (C) or no (R) alteration by soil forming processes. A/C horizons are defined based on the occurrence of bioturbation and relict primary structures. As these properties are typical of both A and C horizons, an A/C horizon represents the combination of an A-type horizon and a C-type horizon (following Buol *et al.*, 2011). Similarly, B/C horizons are composed of beds that contain features of B horizons (slickensides, rhizoliths, fossil traces, incipient soil structure) and preserve characteristics of C horizons (massive or having some primary sedimentary structures).

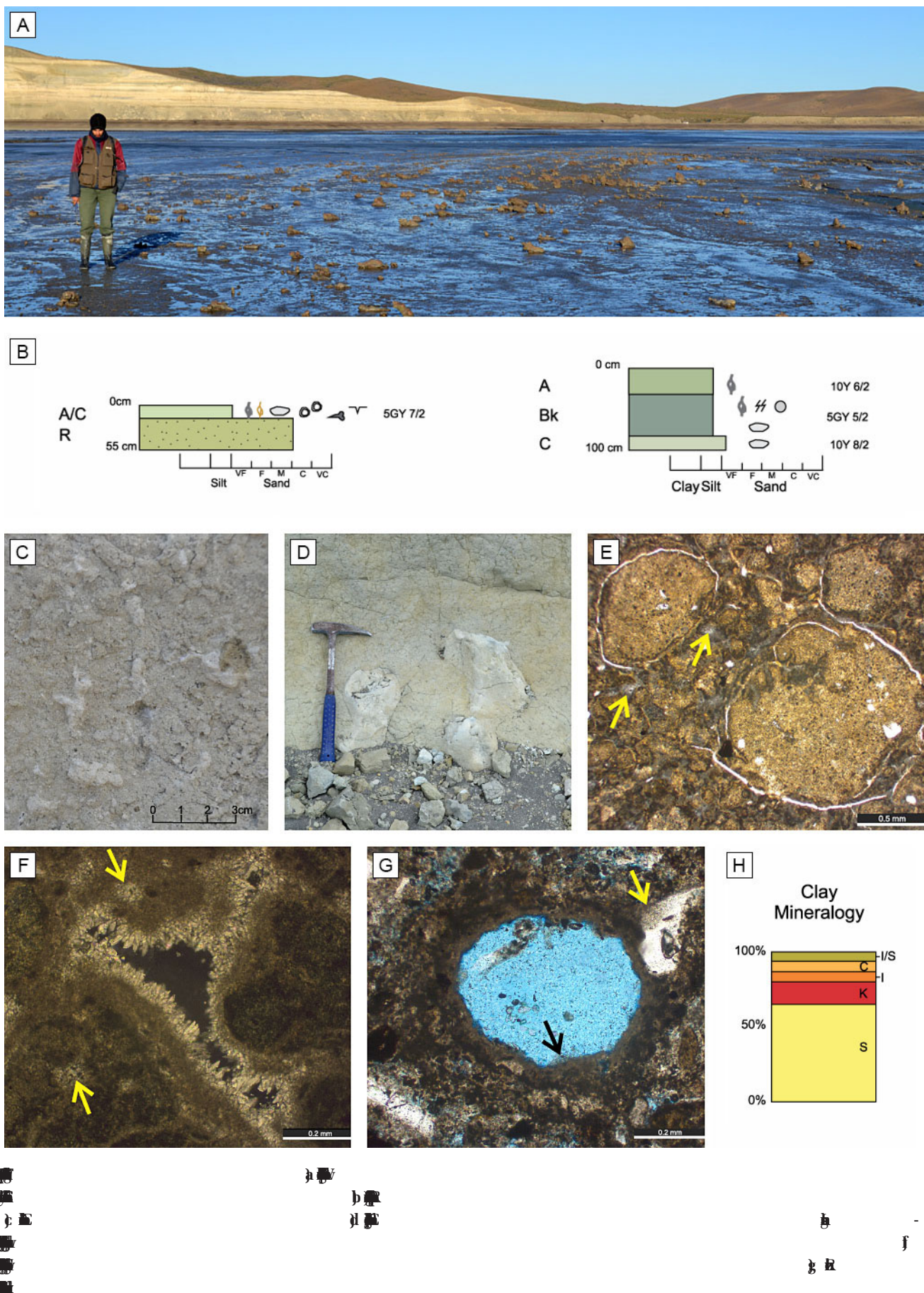
Pedotype 1 (P1a and P1b)

This paleosol type (n=80) is widely represented (69% of all paleosols in the measured sections) in the SCF at the four studied localities (Fig. 2). P1 is developed over light gray (N7), yellowish gray (5GY 7/2), grayish yellow green (5GY 7/2), to pale olive (10Y 6/2) massive silty-clayey facies (Fm) that rarely contain primary sedimentary structures in the form of millimeter-scale planar lamination (Fl facies), massive sandstones (Sm facies), massive tuffs (Tm facies), and tuffs with relict ripples (Tr facies) (Table 1; Figs. 2 and 4). It is characterized as a grayish-greenish paleosol with very weak to weak horizonation with A/C-R (Pedotype 1a; P1a) or B/C-R (Pedotype 1b; P1b) profiles, respectively (Fig. 4B).

Pedotype	Macropedofeatures	Ichnofossils	Microfossil remains	Other features
P1a	Ferric rhizoliths, delicate rhizoliths, massive horizons, relict sedimentary structures	<i>Celliforma roselli</i> , <i>Celliforma argentina</i> , <i>Fictovichnus gobiensis</i> , <i>Feoichnus chall</i> , <i>Taenidium barretti</i>	Exclusive elements: cavate, puzzle and boat-type phytoliths, fragmented and whole sponge spicules, preserved epidermis. Non-exclusive: unicellular, multicellular and eroded phytoliths, charcoals, palynomorphs, radiolarians	Fossil bones
P1b	Ferric rhizoliths, delicate rhizoliths, mottles, incipient soil structure, massive or relict sedimentary structures	<i>Celliforma roselli</i> , <i>Celliforma argentina</i> , <i>Palaeophycus tubularis</i> , <i>Planolites beverleyensis</i>	Exclusive elements: cavate, puzzle and boat-type phytoliths, fragmented and whole sponge spicules. Non-exclusive: unicellular, multicellular and eroded phytoliths, charcoals, palynomorphs, radiolarians	Fossil bones
P2	Calcareous rhizoconcretions, calcareous nodules, Fe-oxides rhizoliths, delicate rhizoliths, slickensides,	Mammal footprints, undifferentiated burrows	Exclusive elements: oblong and tower phytoliths. Non-exclusive: unicellular, multicellular and eroded phytoliths, charcoals, palynomorphs and radiolarians	Desiccation cracks, vertebrate fossil remains
P3	Fe-rich rhizoliths, delicate rhizoliths slickensides, mottles, angular/subangular blocky or wedge-shaped peds	<i>Celliforma roselli</i> , <i>Celliforma argentina</i> , <i>Fictovichnus gobiensis</i>	Exclusive elements: cyperoid elongate, saddle, slightly bilobate, plurilobate and echinate globular phytoliths, stomatocys and diatoms. Non-exclusive: unicellular, multicellular and eroded phytoliths, charcoals, palynomorphs, radiolarians,	Fossil bones







alescent excrements. Rhizocretions (*sensu* Klappa, 1980) around root cavities (pedotubules), coatings of fibre calcite lying perpendicularity to the surface of these root cavities, floating and etched skeleton grains, and bladed calcite coronas are observed at a micro scale (Fig. 5G). Compositionally, the non-clay minerals identified by XRD are, in decreasing order of abundance, calcite, quartz, and feldspars, together with very small amounts of opal. The clay minerals of the P2 (Fig. 5H) are characterized by the dominance of smectite (90–40%), with a lesser amount of illite and illite/smectite mixed-layers (25–5%), kaolinite (<20%), and chlorite (<10%).

Pedotype 3 (P3)

The P3 pedotype (n=16; 14% of the all paleosol profiles in the measured sections) is found in the middle and in the bottom of the lowermost upper part of the SCF (Fig. 2) with low relative abundance. It is developed on pale olive (10Y 6/2) to 5Y 4/4 (moderate olive brown) massive tuffs (Tm facies), massive sandy facies (Sm), massive or laminated silty-clayey facies (Fm and Fl, respectively) (Table 1; Figs. 3 and 6). This pedotype is defined as an olive-colored paleosol with Fe-rich and delicate rhizoliths, *Celliforma rosellii*, *Celliforma argentina*, *Fictovichnus gobiensis*, slickensides, mottles, and angular/subangular blocky or wedge-shaped structure (Fig. 6B–D; Table 2). Fossil mammal and microfossil remains are present in this pedotype (see below and Table 2). This pedotype constitutes profiles with A-Bss1-Bss2-Bss3-C or R, A-Bss, or Bss-C or R horizons (see Fig. 6B for features of each horizon).

At a micro scale (Fig. 6E–H), the coarse fraction of the Bss horizons is made up of quartz, k-feldspars, and plagioclases with low degree of alteration, glass shards (planar and cusped shape) and pumiceous fragments with medium to high degree of alteration (Fig. 6E). In addition, there are volcanic lithic fragments with pilotaxic and trachytic textures with fresh to low degree of alteration (Fig. 6E), and fragments of sedimentary rocks. Grains of amphibole, epidote, biotite, and opaque minerals, as well as phytolithic remains and diatoms also occur in the coarse fraction. The Bss horizon shows fine siltstone to medium sand particle size classes.

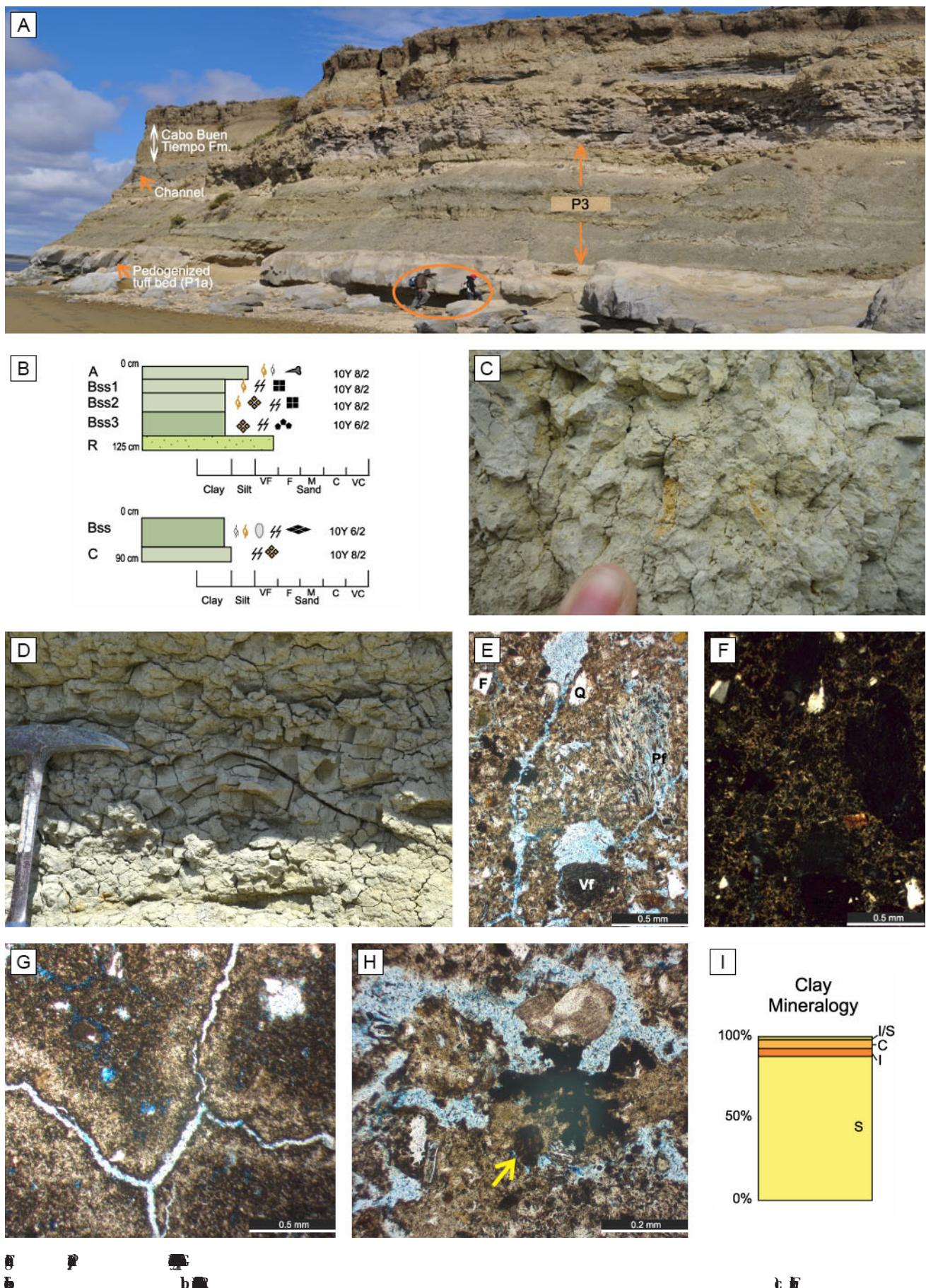
The mineral coarse fraction is composed of medium sand grains. The c/f ratio (c/f = 3.1 μm) ranges from 3/1 to 1/9 with an open to closed porphyric distribution. The groundmass is light to dark brown, probably in part due to the presence of organic matter. The b-fabric is granostriated (Fig. 6F), reticulated, speckled, and undifferentiated. Blocky peds defined by channels and planar voids are common (Fig. 6G). Internal wedge-shaped micropeds, granular micropeds, and angular to subangular blocky micropeds are observed. Compound packing voids, chambers, channels, and vughs are preserved in the groundmass. The pedofeatures are clay coatings and Fe-Mn oxide coatings around wall chambers and channels; loose discontinuous infillings of dark or light groundmass inside chambers and vughs, and dense incomplete infillings of zeolites (clinoptilolite) inside vughs. Also there are coatings; hypocoatings, and quasicoatings of organic matter around planar and channel voids (Fig. 6G); scarce to abundant Fe-Mn oxides and Mn oxides aggregated nodules with amiboidal shape (Fig. 6H) or typic; abundant very porous microaggregates of excrements (Fig. 6H); and scarce pedorelicts or intraclasts.

Non clay minerals determined from XRD analyses are, in decreasing order of abundance, quartz and feldspars with small amounts of opal, clinoptilolite and calcite. Clay minerals consist mainly of smectite (95–80%) with a low proportion of illite (<10%), chlorite (<10%), and illite/smectite mixed-layers (<5%) (Fig. 6I).

MICROREMAINS DATASET OF THE SANTA CRUZ FORMATION

Although the majority of the analysed paleosols (75% of the total samples) preserves phytoliths and microfossil remains, a minor portion of the studied paleosols (25% of the total samples), mainly from P1 and P3, do not present microremains. Within the fertile samples, there are a 15% of samples that do not present sufficient abundance of remains to be considered in the statistical analyses. For this reason, we have been able to describe and compare in-group form only according to the pedotype to which they belong (Fig. 7A; Table 2).

calcite (PN, 10x). h) Average data of clay mineralogy (S: smectite; K: kaolinite; I: illite; C: chlorite; I/S: mixed layers of illite/smectite) in P2. PN: parallel nicols; XN: crossed nicols.



From the comparative analysis of the presence and abundance of the main phytolith morphotypes (Fig. 7B), clear similarities can be observed between the compositions (Fig. 8) of the three pedotypes. This is especially apparent from the greater abundance of elongated elements (Fig. 8R), as well as polyhedral (Fig. 8Q), fan-shaped (Fig. 8P), point-shaped (Fig. 8E), and different globular (Fig. 8C and D) phytoliths. The exclusive presence of particular elements characterizes each pedotype (Table 2). Thus, cavae, puzzle (Fig. 8G), and boat-type (Fig. 8B) phytoliths belong to P1 (Fig. 7 and Table 2) demarcate the presence of dicots and microthermal grasses (C_3 plants). Oblong elements belong to P2 (Fig. 7 and Table 2); while, cyperoid elongate phytoliths belong to P3 (Fig. 7 and Table 2). Tower elements are the dominant form in P2; meanwhile, saddle, slightly bilobate, plurilobate (Fig. 8B), and echinate globular (Fig. 8C) phytoliths are the most abundant elements in P3. This indicates a greater abundance of temperate elements in P2, whereas in P3 there are megathermal elements (C_4 plants) that suggest variable conditions in hydric availability. Multicellular phytoliths (mainly formed by fragments of woody tissue) and eroded phytoliths (Fig. 8M) are also present in the three pedotypes. Similarly, large elements (elongate, polyhedral, and fan-shaped types) with different degree of erosion were also observed. Non-phytolith microremains, such as charcoals (Fig. 8N), palynomorphs (Fig. 8K), and radiolarians (Fig. 8I) occur in all the pedotypes. Stomatocys (Fig. 8L) and diatoms (Fig. 8L) are exclusively present in P3 (Fig. 7 and Table 2). Fragmented and whole sponge spicules (Fig. 8O) characterize P1 (Fig. 7 and Table 2). Particularly, in one sample of the P1, preserved epidermis with siliceous elements has been found (Fig. 7, 8A and Table 2). It has a marked graminoid affinity, with a disposition of zoned epidermal elements (in costal and intercostal areas) with several rows of costal short cells, with elongated saddle-shaped siliceous elements. The intercostal zone has a band of two rows of stomata with low dome-shaped, ovoid,

cells; the width of the subsidiary cells smaller in relation to the horizontal length, and the presence of hooks. Cells in the middle part of the intercostal zone are interrupted by single saddle square short cells. Although this set of characters does not allow the determination of its affinity at a specific level, it demonstrates a clear chloridoid affinity (C_4 plants).

VERTEBRATE-BEARING PALEOSOLS

Vertebrate fossils were recorded in levels of the P2, the middle part of the unit, in the area of Monte Tigre, very near to the Cañadón Las Totoras locality, and at Cañadón Palos (see Figs. 1B and 2). These fossils include mostly rodents, xenarthrans (sloths and cingulates), litopterns and notoungulates (both typotheres and toxodontians) (Table 3). In a preliminary taxonomic approach, taxa collected were similar to those recorded from the best-known northern localities such as Puesto La Costa and Estancia La Costa (Estancia La Costa Member) (e.g., Vizcaíno *et al.*, 2012) (see Fig. 1B). To date, no taxa found in the upper member are absent in the lower member, although the proportions of different mammalian taxa appear to be different.

DISCUSSION

Pedogenesis

Paleosols classification: Very poorly defined soil horizons of the P1a, with scarce macrofeatures (bioturbation), preservation of sedimentary structures, and a low to medium degree of alteration of the coarse components suggest very weak pedogenic modification (e.g., Retallack, 2001). These features are similar to modern Entisols (*i.e.*, immature soils with a very poor degree of development that can have little or no development of pedogenic horizons, following Soil Survey Staff, 1999; Buol *et al.*, 2011; Schoeneberger *et al.*, 2012). Thus, P1a is classified and interpreted as a paleo-Entisol (Retallack, 2001), and as a Protosol

and subangular blocky peds in a Bss horizon. **d)** Conjugate slickensides that define wedge-shaped peds in a Bss horizon. **e)** Microscopic view of the light to dark brown groundmass and the coarse fraction of the P3 showing medium sand particles of volcanic (Vf) and pumiceous (Pf) fragments, quartz (Q) and feldspar (F) (PN, 4x). **f)** Same field as in e showing a granostriated b-fabric (XN, 4x). **g)** Planar and channel voids that defined strongly developed blocky peds (PN, 4x). **h)** Detail of strongly impregnated amiboidal Fe-Mn nodule. The arrow marks an oval microaggregated (excrement) (PN, 10x). **i)** Average data of clay mineralogy (S: smectite; I: illite; C: chlorite; I/S: mixed layers of illite/smectite) in P3. PN: parallel nicols; XN: crossed nicols.

**MONTE TIGRE LOCALITY (CLOSE TO CAÑADÓN
LAS TOTORAS LOCALITY)**

Marsupialia

Sparassodonta indet.

Litopterna

Proterotheriidae indet.

Notoungulata

Typotheria

Interatheriidae

Protypotherium sp.

Hegetotheriidae

cf. *Interatherium*

Toxodontia

Adinotherium sp.

Nesodon sp.

Astrapotheria

cf. *Astrapotherium*

Xenarthra

Cingulata

Glyptodontidae

Propalaeohoplophorinae indet.

Eucinepeltus sp.

Dasypodidae

Prozaedyus sp.

Folivora

Eucholoeops *ingens*

Eucholoeops sp.

Pelecyodon sp.

Nematherium sp.

Rodentia

Erethizontidae

Steiomysduplicatus

Chinchilloidea

Prolagostomus sp.

Cavioidea

Eocardia sp.

Neoreomys sp.

Aves

Cariamidae indet.

CAÑADÓN PALOS LOCALITY

Marsupialia

Abderitidae

cf. *Abderites*

Litopterna

Proterotheriidae indet.

Notoungulata

Toxodontia

Adinotherium sp.

Rodentia

Cavioidea

Neoreomys sp.

Chinchilloidea

Perimys sp.




M et al. 





















































































































































































































































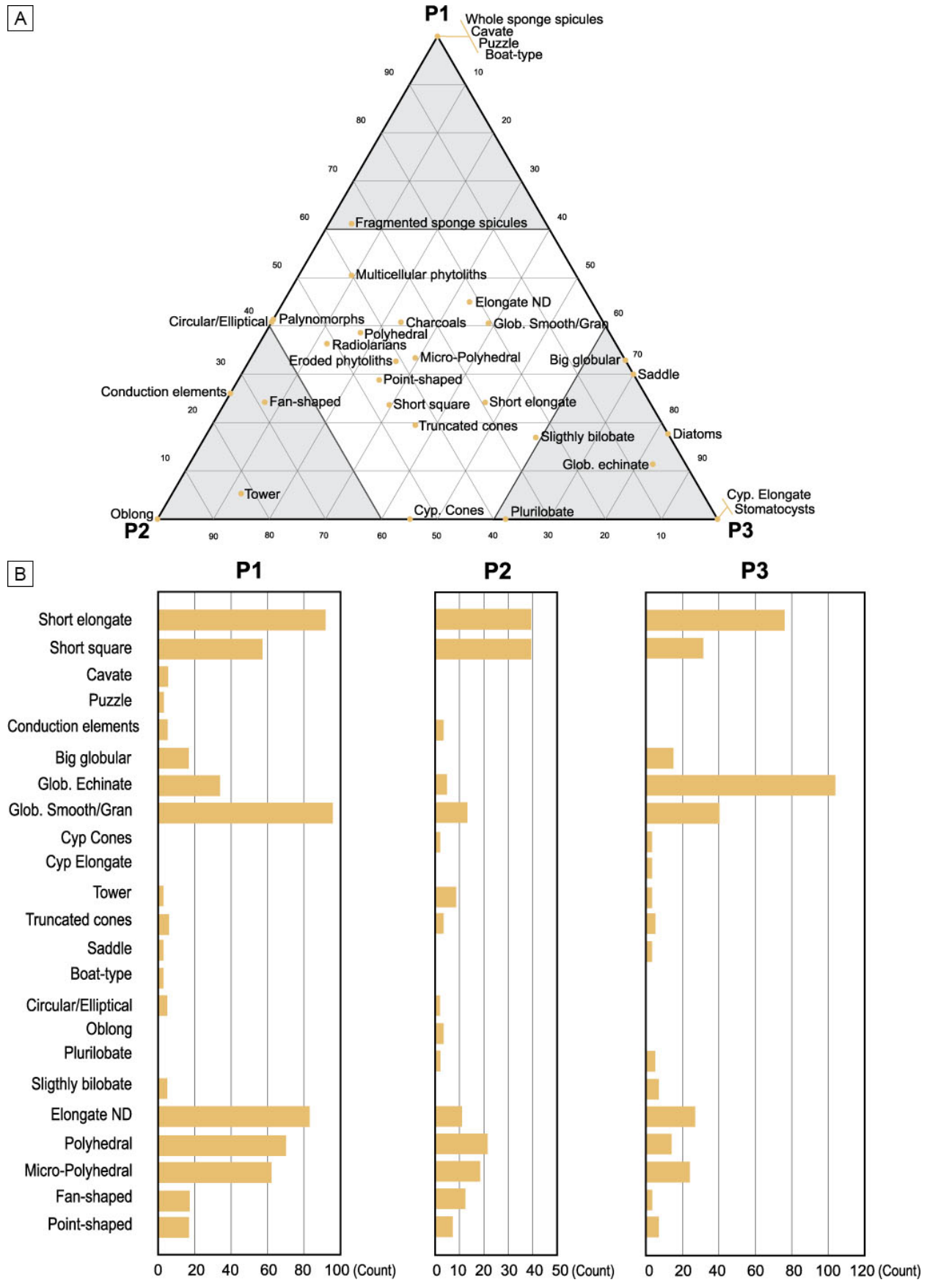


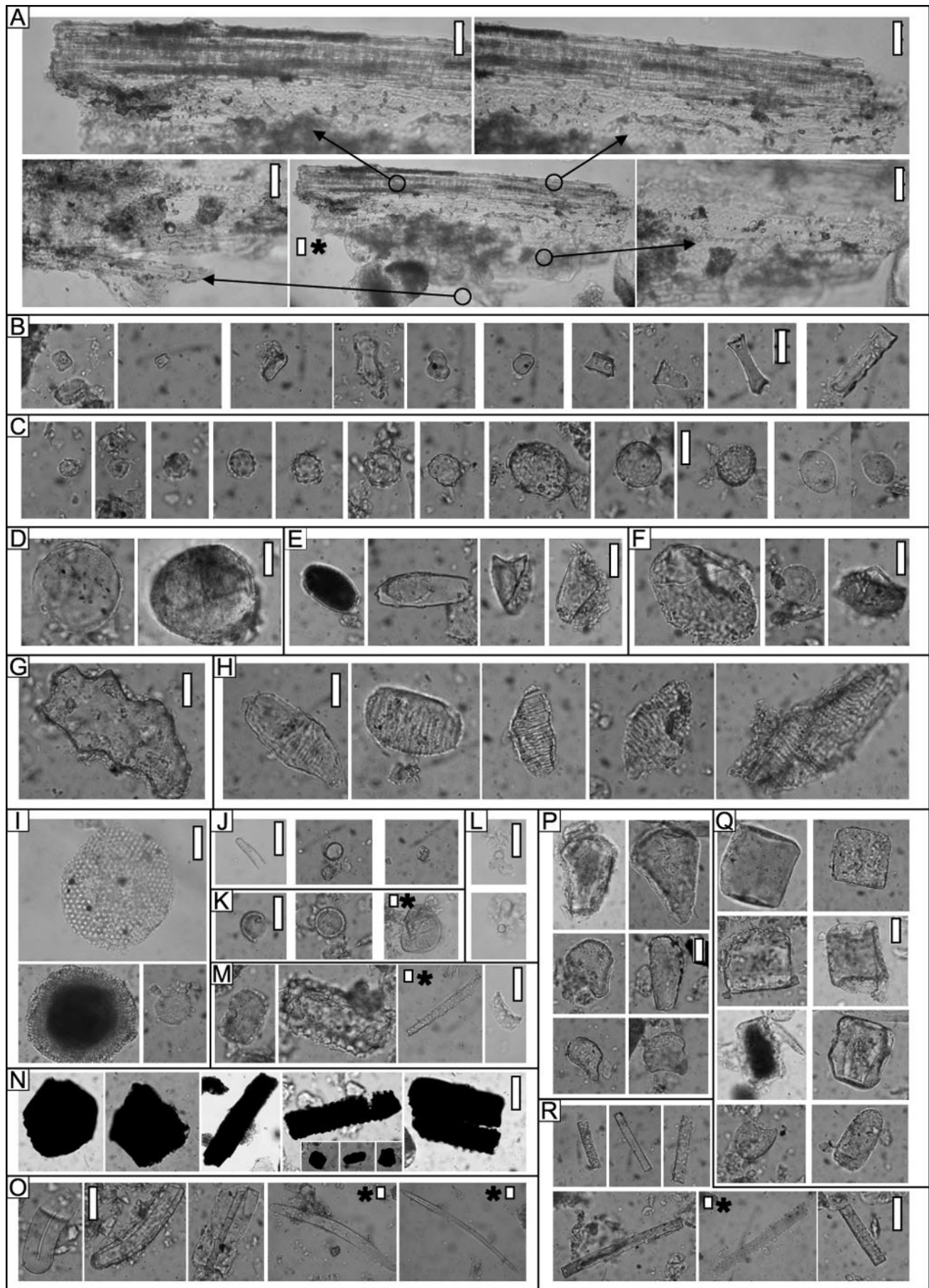


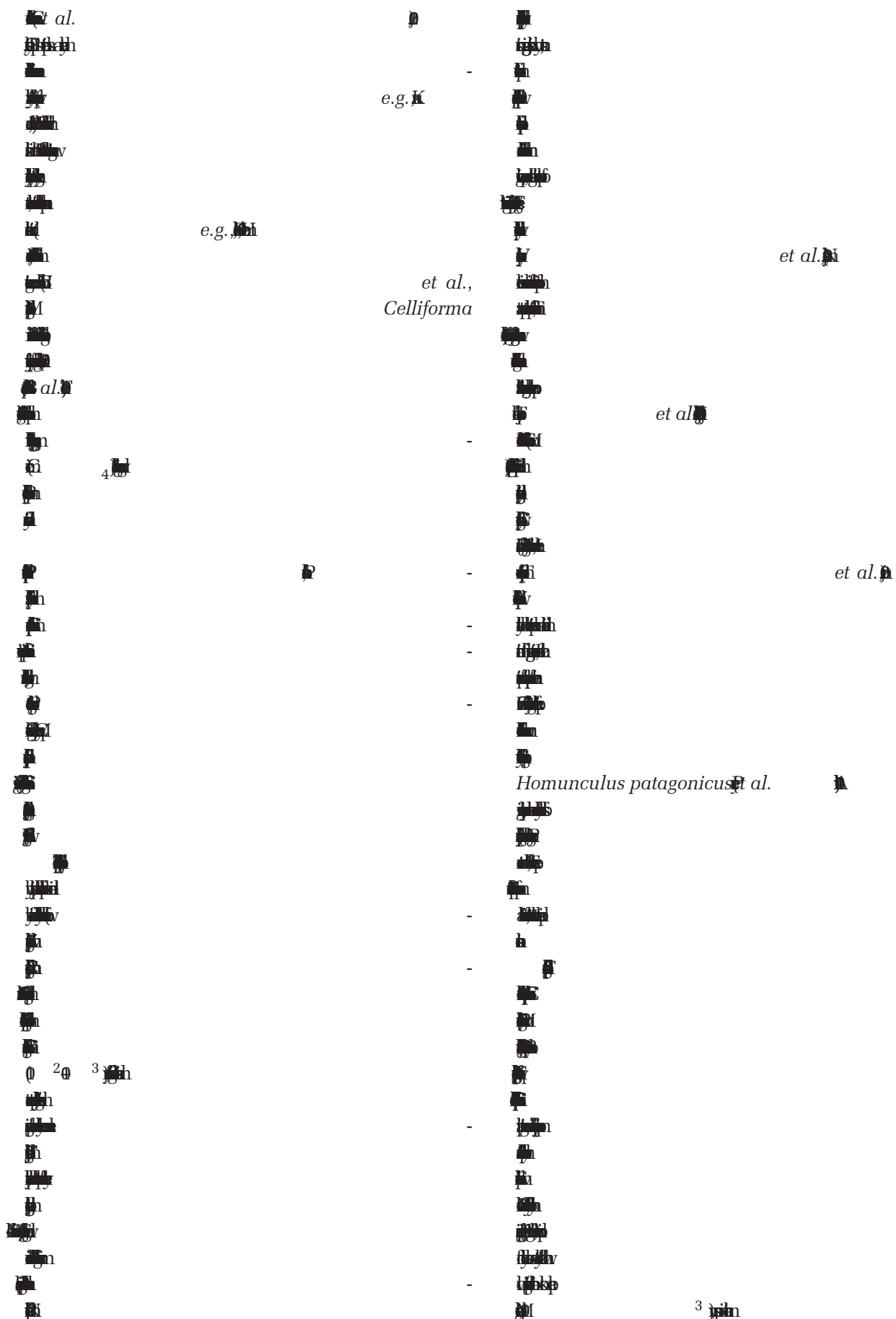








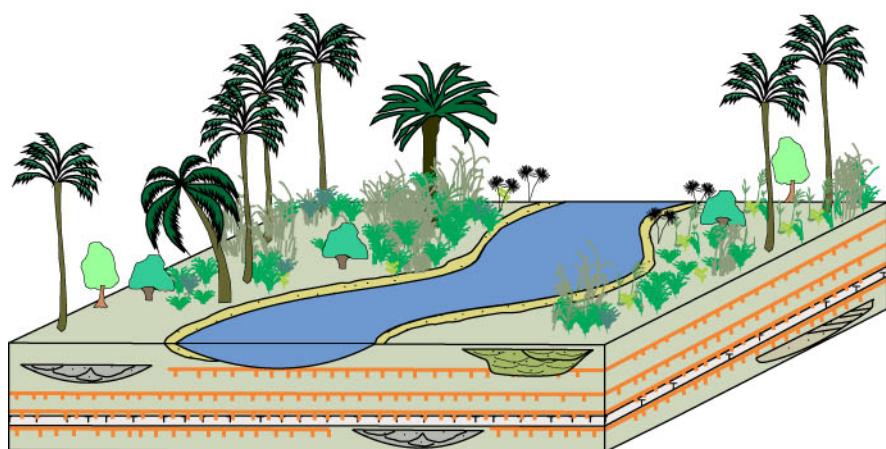
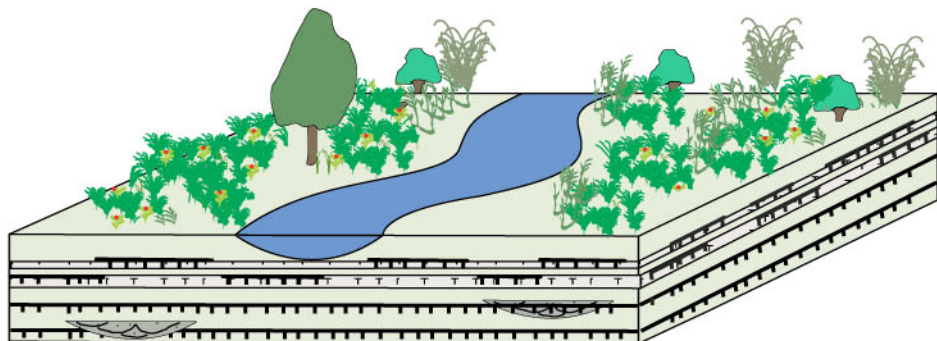
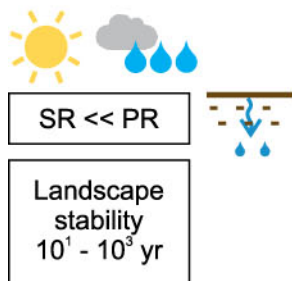




Pedotype	Macro, micro-features and clay mineralogy	Pedogenic processes
P1a	Macro: Rhizoliths, burrows, <i>Celliforma rosellii</i> , <i>Celliforma argentina</i> , <i>Fictovichnus gobiensis</i> , <i>Feoichnus challa</i> , <i>Taenidium barretti</i> Micro: Channels and chambers	
P1b	Macro: Rhizoliths, burrows, <i>Celliforma rosellii</i> , <i>Celliforma argentina</i> , <i>Palaeophycus tubularis</i> , <i>Planolites beverleyensis</i> Micro: Channels and chambers	Bioturbation
P2	Macro: Rhizoliths, mammal footprints, burrows Micro: Excrements and granular peds	
P3	Macro: Rhizoliths, <i>Celliforma rosellii</i> , <i>Celliforma argentina</i> , <i>Fictovichnus gobiensis</i> Micro: Chambers, channel, infillings of groundmass and excrements	
P1a	Dominance of smectite Macro: Blocky, wedge-shaped peds and slickensides	
P1b	Micro: Striated b-fabric and blocky peds Dominance of smectite Macro: Slickensides	
P2	Micro: Striated b-fabric, blocky peds, planar voids, shrinkage and circumgranular porosity Dominance of smectite Macro: Slickensides and blocky structure	Vertization
P3	Micro: Striated b-fabric, planar voids, blocky and wedge-shaped peds Dominance of smectite	
P2	Macro: Calcareous rhizoconcretions and nodules Micro: Crystallitic b-fabric, carbonatic coatings, infillings, nodules, and bladed calcite coronas Rhizocretions, pedotubles, coating of fiber calcite and floating etched grains	Calcification
P1a	Macro: Fe-Mn nodules Micro: Fe-Mn nodules	
P2	Macro: Fe-rich mottles and rhizoliths Micro: Fe-Mn coatings and nodules	Gleization
P3	Macro: Fe-rich mottles and rhizoliths Micro: Fe-Mn coating and Fe-Mn and Mn nodules	
P2	Micro: Clay, carbonatic, Fe-Mn and organic matter coatings	Illuviation
P3	Micro: Clay, Fe-Mn and organic matter coatings, organic matter hypocoatings and quasicoatings	
P1b	Light to dark brown color of the groundmass	
P2	Light to dark brown color of the groundmass and organic matter coatings	Melanization
P3	Light to dark brown color of the groundmass and organic matter hypocoatings, quasicoatings and coatings	
P1b, P3	Pedorelicts	Alluviation

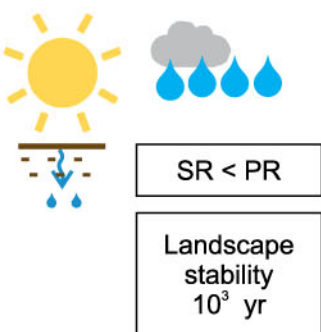
Stage 3

(upper part of the SCF;
upper ELAM)



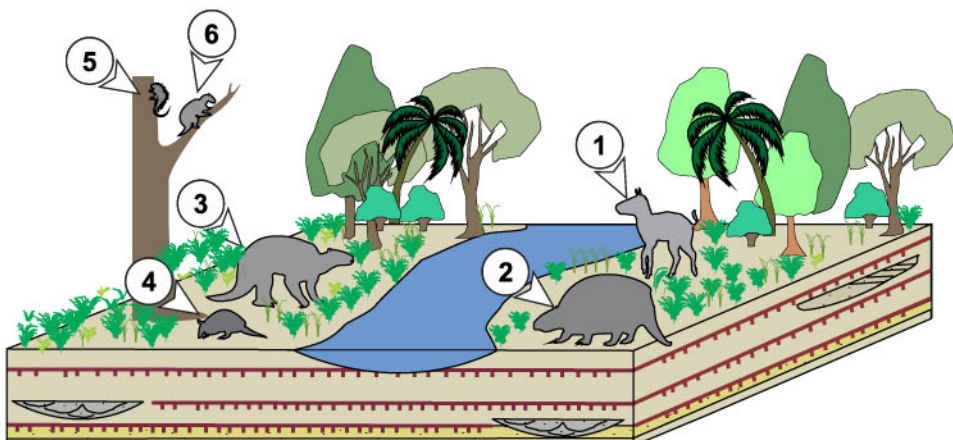
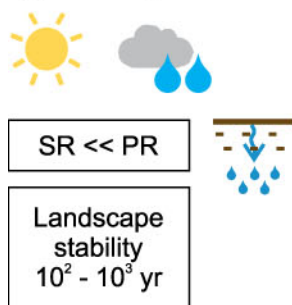
Stage 2

(bottom of the lowermost
upper part of
the SCF; lowermost ELAM)



Stage 1

(middle part of the SCF;
upper ELCM)



Moderate; moderately well-drained soil conditions

Well-drained soil conditions

Increasingly warmer
↓

Confined simple channels

Unconfined simple channels

Confined complex channels

Sandy sheetfloods

Pyroclastic sheetfloods

Epiclastic distal floodplain

Pedotype 3

Pedotype 2

Sporadic

Pedotype 1a, 1b

Pedotype 1a, 1b

1-Litopterna

2-Gliptodonte

3-Prozaedyus

4-Nematherium

5-Steiomys

6-Eucholoeops



in non-pedogenically modified beds up-section (uppermost part of S3) suggest a progressive increase in sedimentation/aggradation rate of the floodplain. This situation reduced the number and the duration of pauses in deposition, and this impeded the progress in pedogenesis. This trend was probably a consequence of a more continuous pyroclastic input and a less favorable climatic context (*i.e.*, drier conditions than at S2) that could have conditioned the vegetation cover and the soil fauna (Zapata, 2018).

CONCLUSIONS

The middle and upper parts (~ 17.0 to 15.9 Ma) of the Santa Cruz Formation in southernmost Patagonia represent a fluvial system dominated by both epiclastic and pyroclastic distal floodplain deposits that contain different stacked paleosols. These are interpreted as similar to modern Entisols (P1a), Inceptisols (P1b), calcic Inceptisols (P2), and Vertisols (P3) that preserve ichnofossils, and fossil flora and vertebrates. The conjunction of abiotic and biotic data of the analyzed successions of the SCF provides multidisciplinary paleoenvironmental interpretations that allow to reconstruct three different terrestrial landscapes.

The first landscape (middle part of the SCF; upper Estancia La Costa Member) represents an epiclastic distal floodplain bearing weakly developed paleosols (P2). These paleosols supported a mixed environment (open areas with patches of trees) in which a diverse, mixed Santacrucian fauna and a scarce soil fauna developed under relatively warm and seasonally humid conditions. Soil conditions were well-drained with fluctuating soil moisture. P2 formed during short time spans (10^2 – 10^3 yr) of insignificant or null sedimentation rate and it represents a relatively high sedimentation/pedogenesis ratio in a relatively continuous aggrading environment.

The second reconstructed landscape (the bottom of the lowermost upper part of the SCF; lower Estancia La Angelina Member) is composed of mainly epiclastic distal floodplain settings with minor pyroclastic proximal areas that contain mainly weakly–mildly developed soils (P3). This landscape supported Vertisols and an ecosystem dominated by grasses and palms adapted to variable conditions in hydric availability (C_4 plants), and a soil mesofauna that characterize moderately well-drained soil conditions with a seasonal relatively high water table.

Moderately-long (10^3 yr) intervals of landscape stability with low sedimentation/pedogenesis ratio in a more distal position of the floodplain, and relatively warm and seasonal humid conditions—with higher moisture conditions—took place to P3.

Finally, the third landscape (upper part of the SCF; upper Estancia La Angelina Member) attests to the existence of an epiclastic and pyroclastic distal and proximal floodplain over which Protosols with a microthermic (C_3 plants) herbaceous vegetation, and a soil mesofauna formed under moderately well-drained and moderately-drained soil conditions. P1a and P1b developed during very short–short periods of pedogenesis (10^1 – 10^3 yr) with high ratios of sedimentation/pedogenesis, under a relatively warm and seasonal humid climate, slightly more humid or less seasonal than the climate inferred for the first landscape. Towards the end of the unit, sporadically Protosols developed (P1a and P1b). Although these paleosols represent environmental and ecological conditions similar to those of the lower part of this landscape, a reduction in the number and duration of pauses in deposition, a more continuous volcanoclastic input, and relatively drier conditions characterized the last part of this landscape.

The succession of these different paleolandscapes took place under fluctuating environmental and climatic conditions, in the context of a highly aggrading fluvial system, under relatively warm and humid conditions with variable water availability. The rate of sediment supply, the input of pyroclastic materials, the position on the floodplain, the duration of landscape stability (*i.e.*, pedogenesis time), the alternations of wetter and drier climate phases, and the changes in local hydrologic conditions controlled the soil mesofauna, the vegetation cover, the pedogenic processes, the types of soils, and the degree of soil development.

Acknowledgments

Financial and logistical support for these studies was provided by the projects PIP 100523 of the CONICET (to MSR), and NSF BCS-1749307 (to JMGP). The suggestions made by the reviewers P. Bouza and E. Bedatou, and by the Invited Editor J.I. Cuitiño, greatly improved the quality of this manuscript. The authors would like to thank S. Matheos (CONICET, Argentina), R. Kay (Duke University, USA), M.S. Bargo (CIC, Argentina) and S. Vizcaíno

(CONICET, Argentina) for financial and logistical support, and A. Larroca (UNLP, Argentina), and J. Zuazo and N. Muñoz (CONICET, Argentina) for their assistance during field trips.

REFERENCES

Alonso-Zarza, A.M., and V.P. Wright, 2010. Calcretes. In: A.M. Alonso-Zarza and L.H. Tanner (Eds.), *Carbonates in Continental Settings: Facies, Environments and Processes*. Elsevier, Amsterdam, 225-267.

Alonso-Zarza, A.M., M.E., Sanz, J.P. Calvo, and P. Estévez, 1998. Calcified root cells in Miocene pedogenic carbonates of the Madrid Basin: evidence for the origin of Microcodium b. *Sedimentary Geology* 16:81-97.

Ashley, G., and S. Driese, 2000. Paleopedology and paleohydrology of a volcanoclastic paleosol interval: implications for Early Pleistocene stratigraphy and paleoclimate record, Olduvai Gorge, Tanzania. *Journal of Sedimentary Research* 70:1065-1080.

Badawy, H.S., 2017. Termite nests, rhizoliths and pedotypes of the Oligocene fluviomarine rock sequence in northern Egypt: Proxies for Tethyan tropical palaeoclimates. *Palaeogeography, Palaeoclimatology, Palaeoecology* 492:161-176.

Barboni, D., and L. Bremond, 2009. Phytoliths of East African grasses: An assessment of their environmental and taxonomic significance based on floristic data. *Review of Palaeobotany and Palynology* 158:29-41.

Bargo, M.S., N., Toledo, and S.F. Vizcaíno, 2012. Paleobiology of the Santacrucian sloths and anteaters (Xenarthra, Pilosa). In: Vizcaíno, S.F., Kay, R.F. and M.S. Bargo (Eds.), *Early Miocene Paleobiology in Patagonia: high-latitude paleocommunities of the Santa Cruz Formation*. Cambridge University Press, Cambridge, UK, 216-242.

Bellosi, E.S., and M.G. González, 2010. Paleosols of the middle Cenozoic Sarmiento Formation, central Patagonia. In: Madden, R.H., Carlini, A.A., Vucetich, M.G., and R.F. Kay (Eds.), *The Paleontology of Gran Barranca: Evolution and Environmental Change through the Middle Cenozoic of Patagonia*. Cambridge University Press, Cambridge, UK, 293-305.

Bertels, A., 1970. Sobre el "Piso Patagoniano" y la representación de la época del Oligoceno en Patagonia Austral, República Argentina. *Revista de la Asociación Geológica Argentina* 25: 496-501.

Biddle, K., M., Uliana R. Jr., Mitchum, M., Fitzgerald, and R. Wright, 1986. The stratigraphic and structural evolution of central and eastern Magallanes Basin, Southern America. In: P. Allen and P. Homewood (Eds.), *Foreland basins*. International Association of Sedimentologists, Special Publication 8:41-61.

Billings, E., 1862. New species of fossils from different parts of the Lower, Middle and Upper Silurian rocks of Canada. In: *Palaeozoic Fossils* (Vol. 1, 1861-1865). *Geological Survey of Canada Advance Sheets*. Canadá, 96-168.

Birkeland, P., 1999. *Soils and geomorphology*. Oxford University Press, New York, 430 pp.

Bradshaw, M.A., 1981. Palaeoenvironmental interpretations and systematics of Devonian trace fossils from the Taylor Group (Lower Beacon Supergroup), Antarctica. *New Zealand Journal of Geology and Geophysics* 24:615-652.

Brea, M., A.F., Zucol, and A. Iglesias, 2012. Fossil plant studies from late early Miocene of the Santa Cruz Formation: paleoecology and paleoclimatology at the passive margin of Patagonia, Argentina. In: Vizcaíno, S.F., Kay, R.F. and M.S. Bargo (Eds.), *Early Miocene Paleobiology in Patagonia: high-latitude paleocommunities of the Santa Cruz Formation*. Cambridge University Press, Cambridge, UK, 104-128.

Brea, M., A.F., Zucol, M.S., Bargo, J.C., Fernicola, and S.F. Vizcaíno, 2017. First Miocene record of Akaniaceae in Patagonia (Argentina): a fossil wood from the Early Miocene Santa Cruz Formation and its palaeobiogeographical implications. *Botanical Journal of the Linnean Society* 183:334-347.

Bromley, R.G., 1996. *Trace Fossils: Biology, Taphonomy and Applications*. 2nd Edition, Chapman and Hall, London, United Kingdom, 361 pp.

Bullock, P. N., Fedoroff, A., Jongerius, G., Stoops, and T. Tursina, 1985. *Handbook for soil thin section description*. Waine Research Publications, 152 pp.

Buol, W.S., R.J., Southard, R.C., Graham, and P.A. McDaniel, 2011. *Soil genesis and classifications*. 6th Edition, Wiley-Blackwell, Oxford, 543 pp.

Candela, A.M., and M.B.J. Picasso, 2008. Functional anatomy of the limbs of Erethizontidae (Rodentia, Caviomorpha): indicators of locomotor behaviour in Miocene porcupines. *Journal of Morphology* 269:552-593.

Candela, A.M., L.L., Rasia, and M.E. Pérez, 2012. Paleobiology of Santacrucian Caviomorph rodents: a morpho-functional approach. In: Vizcaíno, S.F., Kay, R.F. and M.S. Bargo (Eds.), *Early Miocene Paleobiology in Patagonia: high-latitude paleocommunities of the Santa Cruz Formation*. Cambridge University Press, Cambridge, UK, 287-305.

Cassini, G.H., 2013. Skull geometric morphometrics and Paleoenvironment of Santacrucian (late Early Miocene; Patagonia) native ungulates (Astrapotheria, Litopterna, and Notoungulata). *Ameghiniana* 50:193-216.

Catena, A.M., D.I., Hembree, B.Z., Saylor, F., Anaya, and D.A. Croft, 2016. Paleoenvironmental analysis of the Neotropical fossil mammal site of Cerdas, Bolivia (middle Miocene) based on ichnofossils and paleopedology. *Palaeogeography, Palaeoclimatology, Palaeoecology* 459:423-439.

Catena, A.M., D.I., Hembree, B.Z., Saylor, F., Anaya, and D.A. Croft, 2017. Paleosol and ichnofossil evidence for significant Neotropical hábitat variation during the late middle Miocene (Serravallian). *Palaeogeography, Palaeoclimatology, Palaeoecology* 487:381-398.

Cecil, C.B., and F.T. Dulong, 2003. Precipitation models for sediment supply in warm climates. In: Cecil, C.B., and N.T. Edgar (Eds.), *Climate Controls on Stratigraphy*, vol. 77. SEPM Special Publication, 21-27.

Collura, L.V., and K. Neumann, 2017. Wood and bark phytoliths of West African woody plants. *Quaternary International* 434 (Part B): 142-159.

Counts, J.W., and S. Hasiotis, 2009. Neochnological experiments with masked chafer beetles (Coleoptera: Scarabaeidae): implications for backfilled continental trace fossils. *Palaios* 24:74-91.

Crifò C., M.S., Bargo, R.F., Kay, M.J., Kohn, S.F., Vicaíno, A.F., Zucol, and C.A.E. Strömberg, 2016. Using phytolith to track vegetation changes during the MMCO of the Santa Cruz Formation, Patagonia (Argentina). *XIV International Palynological Congress - X International Organization of Palaeobotany Conference*.

Crifò C., M.S., Bargo, J.I., Cuitiño, R.F., Kay, M.J., Kohn, R.B., Trayler, S.F., Vizcaíno, A.F., Zucol, and C.A.E. Strömberg,

